Current Research in Geoscience

Research Article

Assessment of Soil Loss Using GIS and RUSLE Model in Bakiya River Basin (BRB), Central Nepal

[1]Sujan Bista, [1]Naresh Kazi Tamrakar, [1]Kishor Rimal and [2]Arju Bhattarai

[1]*Central Department of Geology, Tribhuvan University, Nepal*
[2]*Department of UNIGIS, University of Salzburg, Austria*

Article history
Received: 18-01-2025
Revised: 03-03-2025
Accepted: 14-03-2025

Corresponding Author:
Sujan Bista
Central Department of Geology,
Tribhuvan University, Nepal
Email: sujan.bista14@outlook.com

Abstract: Soil erosion is the major geological hazard in the fragile landscape of Sub-Himalaya. This study examines the susceptibility of the Bakiya River Basin (BRB) in Central Nepal to soil erosion because of its steep topography, fragile geology, the impact of intense monsoon rainfall, and the lack of a direct monitoring mechanism available for rainfall-runoff. This study examines the spatial variations of soil erosion across the basin with the integration of the Revised Universal Soil Loss Equation (RUSLE), Remote Sensing (RS), and Geographic Information System (GIS). The findings identified the areas vulnerable to soil erosion, which are primarily influenced by the topography. The erosion rates in BRB vary from 0 to 729.6 $t.ha^{-1}.yr^{-1}$, with an average erosion rate of 41 $t.ha^{-1}.yr^{-1}$. Furthermore, about 65% of the total area needs immediate conservation action, which exceeds the threshold of 25 $t.ha^{-1}.yr^{-1}$. Model validation using the ROC curve yielded an AUC value of 0.827 which indicates a "Good" accuracy classification for the erosion estimates. The study's findings provide valuable information for conservation planning. They could prove valuable for the proposed and ongoing critical projects such as the Kathmandu Terai Fast Track (KTFT) and Nijgadh International Airport. Erosion control in the BRB is critical for the productivity of soil and environmental protection, as well as for minimizing downstream impacts such as sedimentation, flooding, and soil degradation. This study emphasizes the importance of sustainable management approaches in preserving the basin's soil and economic feasibility.

Keywords: RUSLE Model, Siwalik, Soil Loss, NDVI, Bakiya River, ROC-AUC

Introduction

When soil particles are displaced from their original position to a location farther downstream by external agents like water and wind, this is called soil erosion. The erosion process helps shape and form the landscapes over time. This process involves the detachment and movement of weathered material, resulting in material removal from the surface. It subsequently delivers sediment to the drainage system, forming zones of erosional or depositional processes. Erosive actions are prevalent in mountainous terrains, whereas depositional processes occur in floodplain areas. However, it is worth noting that both processes can coexist simultaneously in any given environment. For instance, sediment transported from the uplands can be deposited down the valley, and conversely, stream channels can erode sediment within floodplain areas (Morris & Fan, 1998). The causes of soil erosion, such as wind or water, the locations where it occurs (such as splash, sheet, rill, gully, or channel erosion), or the mechanism of erosion may all be used to categorize erosion (Morgan, 2009). Soil erosion causes major problems both onsite and offsite, with costly impacts. It reduces soil fertility and depth, making land less productive and increasing the need for fertilizer on agricultural land, while it leads to sediment buildup in rivers, reservoirs, and irrigation systems, increasing flood risks and damaging infrastructures in the offsite areas (Morgan, 2009).

The Himalayas are the most prominent orogenic belts, and they are a result of the continental convergence of the Indian and Eurasian plates. There is an interrelationship between climate, tectonics, and erosion, which has been a significant scientific discussion over the centuries (Duncan *et al.*, 1998; Olen *et al.*, 2015; Thiede *et al.*, 2004). The highest mountain range in the world is swiftly and actively uplifting and eroding. The Indian Seasonal Monsoon (ISM), between June and

September, delivers large amounts of rainfall to the Himalayas (about 80% of annual precipitation), mainly on the southern front due to the topographic barriers (Andermann *et al.*, 2012; Bohlinger & Sorteberg, 2018; Shrestha, 2000). ISM drives high discharge events and sediment fluxes towards the Indo-Gangetic foreland basin (also called the active Himalayan foreland basin) (Andermann, *et al.*, 2012). The Sub Himalaya or Siwalik range is a geologically young mountain range. It represents one of the largest accumulations of foreland sediments in the world, consisting of fluvial deposits from Neogene to Quaternary (Kizaki, 1994; Tokuoka, 1992; Upreti, 1999). These rocks are very fragile, easily weathered, and disintegrate quickly (Dhital, 2015). In general, the Siwalik region is prone to intense erosion because of its steep terrain, less indurated rocks and minimal soil cover (Galay, 1987; Shrestha *et al.*, 2008). Due to high geomorphology, the sediments mobilize under the influence of surface runoff. Furthermore, these landforms are affected by landslides, debris flows, and rill erosion, which consequently make lowlands, especially Terai plains, more prone to floods, inundation, and sediment deposition (Bhandari & Dhakal, 2019; Dahal *et al.*, 2010; Devkota & Bhattarai, 2011; Tamrakar, 1999; Tamrakar & Yokota, 2008). The interest in mapping spatial variations of soil erosion is growing with the increase of observational data (Cook, 1937). This led to the development of a quantitative soil erosion model based on climate, soil, vegetation, and topography. For more than half a century, a range of erosion models including qualitative, semi-quantitative and quantitative types have been introduced worldwide to quantify soil erosion processes at various scales in space and time (Batista *et al.*, 2019; Nearing, 2013; Terranova *et al.*, 2009). The complexity of the models, the range of processes they operate, and the type of datasets necessary for both model calibration and application differentiate all the developed erosion models. The most widely accepted model is the Universal Soil Loss Equation (USLE) (Wischmeier, 1965) and its updated version, the Revised Universal Soil Loss Equation (RUSLE) (Renard *et al.*, 1991). It is an empirical model that can be combined with Remote Sensing (RS) and geographic information systems (GIS), offers an affordable and efficient method to predict and map soil erosion variations. (Gitas *et al.*, 2009; Lu *et al.*, 2004; Millward & Mersey, 1999). RUSLE estimates soil loss in watersheds where parameters such as hydroclimatic conditions, sediment yields, and other basin characteristics are ungauged (Angima *et al.*, 2003) as well as generates spatial variations of soil erosion (Yue-Qing *et al.*, 2008). Due to its convenient application, RUSLE has been used by researchers to study erosion hazards in several watersheds of Nepal (Ban *et al.*, 2016; Chalise *et al.*, 2018; Ghimire *et al.*, 2013; Koirala *et al.*, 2019; Uddin *et al.*, 2016).

In this context, the present study attempts to identify and analyze the spatial patterns of soil erosion in the Bakiya River Basin (BRB), Central Nepal, where no rainfall-runoff gauges have been installed by the Department of Hydrology and Meteorology, while also examining the key factors responsible for the high rate of erosion. Bakiya River Basin (BRB), originating from the Mahabharat range in the north, is concerned about developmental activities of national interest. The ongoing construction of the Kathmandu Terai Fast Track (KTFT), which is supposed to connect eastern and western Nepal to Kathmandu swiftly, traverses the N-S direction of this basin. Similarly, the Madan Bhandari Lok Marga, Kanti Raj Path highway also traverses this basin; a few km south of its southern vicinity of Nijgadh, the Mahendra highway traverses in an EW direction. The proposed site for the Nijgadh International Airport is situated just a short distance south of the BRB. The geology of the Bakiya River Basin and its associated topography, including steep topography and land use, monsoon precipitation, and seismicity, are the factors determining erosion susceptibility in this area, which in turn implies the flash flood, bank erosion, river shift, course change, and inundation events in the lowland (Ghimire & Timalsina, 2020). The landslides and flood hazard assessment in the Bakiya River Basin (Ghimire & Timalsina, 2020; Pokhrel *et al.*, 2013) have raised a serious question about the loss of sediments from the basin.

Furthermore, the President Chure Terai Madhesh Conservation Development Board's master plan (PCTMCDB, 2017) classified the BRB among the most erosion-prone in the Siwalik. Therefore, this study aims to (1) assess the distribution of soil erosion across BRB through the application of RUSLE Model, GIS and remote sensing methods, (2) identify primary drivers controlling soil erosion in the area, and (3) provide recommendations for effective conservation and land use plannings. The findings will be valuable for policymakers and stakeholders involved in infrastructure development and environmental conservation.

Study Area

Most of the study area falls in the Makawanpur district of Bagmati province, and its small portion is under the Bara district of Madesh province, Central Nepal (Figure 1). The basin spans approximately 322.19 square kilometers and has a 104 km circumference. The study area is geographically situated between approximately 85°5'0" E to 85°20'0" E longitude and 27°13'37" N to 27°28'37" N latitude. From a bird's-eye view, the study area is 58 Km SW of Kathmandu, Nepal's capital city.

The study area comprises varying topography, with the central and southern belts having comparatively flat landscapes and the northern belt having steep terrain. The vast Indo-Gangetic Plain, located at the mountains' foothills, defines the southern belt. Elevations within the area range from 170 meters in the Nijgadh vicinity to over 2000 meters in the northern Tikachuli hill.

Bakiya River is a tributary of the Bagmati River, with its confluence two Km west of Adouri, Bihar. Simat Khola, Lohajor Khola, Majhi Khola, Juina Khahre, Harda Khola, and Hiramani Khahare are some of the significant affluent streams of the Bakiya River. The drainage pattern of the southern belt of the watershed shows a trellis drainage pattern, and that of the northern exhibits a dendritic drainage pattern. From a broader perspective, the watershed shows a dendritic pattern. Based on Strahler (Strahler, 1952), the Bakiya River is of seventh order.

The region falls under subtropical monsoon climatic zone and records an average yearly precipitation of 2153 mm. An analysis of monthly rainfall patterns reveals the distinctive trend in the study area. June, July, August, and September experienced a notable high rainfall accumulation. These months collectively help determine the local climate and hydrology. On the other hand, the remaining months of the year experience relatively less precipitation. The area shows significant seasonal variation, shifting from wet to dry within a year. Lower rainfall months significantly impact ecosystem dynamics, agricultural practices, and the management of water resources, all of which shape the total amount of water available.

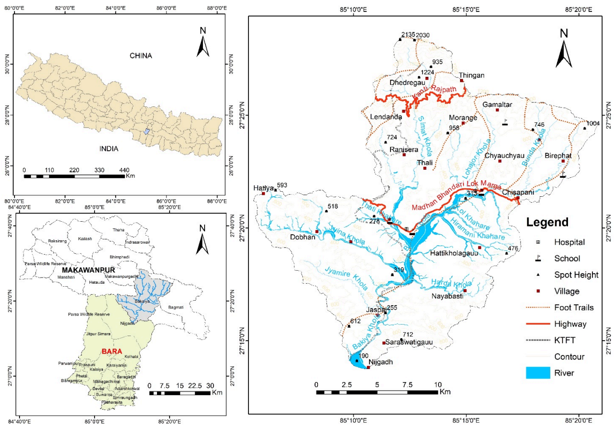

Fig. 1: Location and accessibility map of the study area

Geology of the BRB

The Bakiya River originates in the Mahabharat Range. It flows through a sequence of geological units, including the Lesser Himalaya, Pre-Siwalik, and Siwalik Groups, before reaching the alluvial plains of the Indo-Gangetic Foreland. The large portion of Bakiya River flows through the Siwalik Group, which features sedimentary rocks of fluvial origin from the Middle Miocene to Lower Pleistocene. The Main Frontal Thrust (MFT) marks the boundary between the Siwalik Group and the Quaternary deposits of the Indo-Gangetic Plain, characterized by alluvium boulders, gravel, sand, silt, and clay. To the north, the Main Boundary Thrust (MBT) separates the Siwalik Group from the Precambrian meta-sedimentary and metamorphic rocks of the Lesser Himalayan Sequence. In the central part of the area, the Marin Khola Thrust (MKT) runs almost parallel to the MBT, dividing the Siwalik Group into HFT-MKT and MKT-MBT belts. The upper boundary of the MKT further separates the Siwalik from the overlying Pre-Siwalik Group. All the major faults and folds prevailing in the BRB (Figure 2) are, by their nature, vulnerable to erosion. These are the areas of instability that could generate earthquakes of high magnitude, causing slope instability and consequently delivering sediments to the river channels.

The Siwalik Group is litho-stratigraphically divided into three subgroups in ascending order: Lower Siwalik, Middle Siwalik, and Upper Siwalik. The Lower Siwalik is characterized by variegated mudstone, greenish-grey siltstone, and fine- to medium-grained grey sandstone with occasional marl beds. The Middle Siwalik is divided into two members (Figure 2). Lower Middle Siwalik (MS1) comprises fine- to medium-grained sandstone interbedded with siltstone and mudstone. Upper Middle Siwalik (MS2) is characterized by medium- to coarse-grained sandstone, pebbly sandstone with siltstone, mudstone, and relict sandstone. The Upper Siwalik, confined within the HFT-MKT belt, consists of a matrix-supported conglomerate with subordinate sandstone and mudstone.

The Lohajor Formation of the Pre-Siwalik Group consists of fine- to medium-grained, ripple-marked, pink- to purple-colored sandstone intercalated with minor shale/slate. In the Lohajor River section, bed thickness ranges from a few tens of centimeters up to 0.4 meters. Basic intrusive rocks are also present within this formation (DMG, 2002). The Precambrian metasedimentary rocks characterize the study area's northernmost part and comprise a black-colored slate with intercalations of phyllite, quartzite, and dolomite.

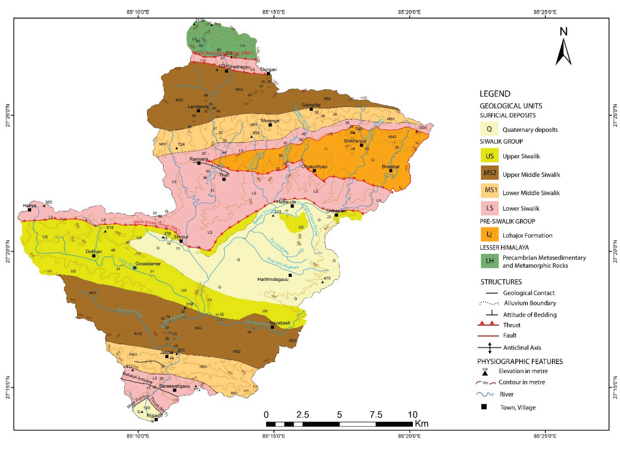

Fig. 2: Geological Map of the Bakiya River Basin (modified after DMG, 2002)

Materials and Methods

The study's methodological framework consists of desk review, data acquisition, analysis and interpretation, and documentation in order. Data sets required to conduct this study include precipitation from different meteorological stations, soil type, Digital Elevation Model (DEM), land use, and crop management (Table 1). Global Positioning System (GPS), Topographic Map, Geological Hammer, Sieves of different sizes, and meter tape were used to collect data in the field. The required data types were divided into primary and secondary data based on accessibility. The soil type, crop management, and geological data are the primary data for the study, whereas the rest falls under secondary data. Figure 3 illustrates the methodological framework adopted in this study.

Table 1: Datasets with their description and their sources used in the study

SN	Data Type	Description	Source
1.	Topographic Map (including Shapefile)	Topo Sheets No. 278513B, 278509B, 278510A, 278510C, 278509C, 278509D were used for watershed delineation, data collection of soil and geology	Government of Nepal, Survey Department
2.	Monthly Rainfall	Monthly rainfall data of 5 weather stations in and around the watershed from the year 2001 to 2022.	Government of Nepal, Department of Hydrology and Meteorology
3	Digital Elevation Model (DEM)	Spatial resolution of 12.5 m was used for the calculation of topographic factors.	ALOS PALSAR
4.	Satellite Imageries	Spatial resolution of 10m was used for the calculation of Normalized Vegetation Index (NDVI)	Sentinel 2, Google Earth Engine
5.	Land Use and Land Cover	Spatial resolution of 10m with accuracy assessment of 80%	Sentinel 2, ESRI Global Database

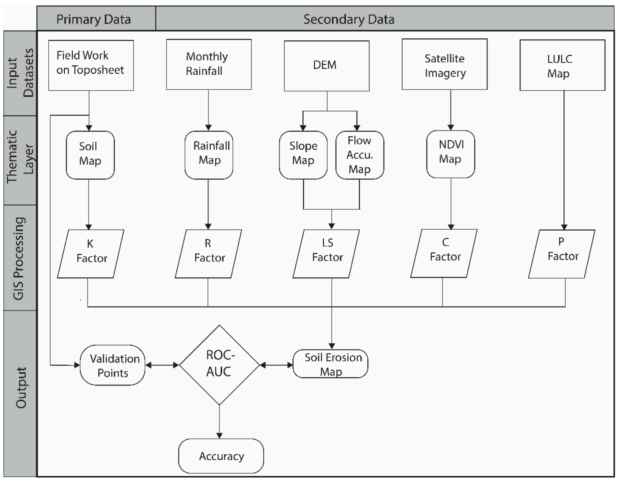

Fig. 3: Flowchart describing methodological framework of RUSLE parameter estimation

RUSLE Parameter Estimation

RUSLE is the widely employed empirical method for predicting erosion rates in a watershed over a prolonged rill and inter-rill erosion period. It can be combined with parameters derived from DEM and LULC, satellite images, such as slope and aspect. The current study began by delineating the BRB from a Department of Survey toposheet at a scale of 1:25,000, using ArcGIS software, followed by an extraction of different RUSLE parameters. The average annual erosion based on RUSLE, expected in the field slope, is computed using Eq. (1).

$$A = R \times K \times LS \times C \times P \quad (1)$$

Where:

A = computed average soil loss in metric tons per hectare per year ($t.ha^{-1}.yr^{-1}$)

R = rainfall-runoff erosivity factor expressed in $MJ.mm.ha^{-1}.h^{-1}.yr^{-1}$

K = soil erodibility factor expressed in $t.h.MJ^{-1}.mm^{-1}$

L = slope length factor

S = slope steepness factor

C = cover management factor

P = support practice factor

In Eq. (1), all the four later factors are dimensionless quantities. All the input layers of varying spatial scales were standardized to a consistent 20-meter spatial resolution using resampling tool in Arc GIS. This spatial harmonization enabled grid-based calculations and minimized distortions caused by the differences in resolutions.

Rainfall Erosivity Factor (R)

The R-factor reflects both the intensity of rainfall and its capacity to generate runoff that can lead to soil erosion (Renard *et al.*, 1991). Estimating R factor requires detailed pluviograph data recorded at interval of 30 minutes or less over a period of at least 20 years to reflect rainfall variability (Renard *et al.*, 1991; Wischmeier, 1965). However, in many parts of the world, including Nepal, obtaining this kind of data can be difficult and time-consuming (Sholagberu *et al.*, 2016; Li & Ye, 2018). Therefore, several studies around the globe have demonstrated a good relationship between yearly rainfall and R-factor (Bonilla & Vidal, 2011). Due to unavailability of rainfall intensity and erosivity records for BRB, the study employs Modified Fourier Index (MFI) (Arnoldus, 1977) using Eq. (2) (Arnoldus, 1977; Prasannakumar *et al.*, 2011; Wischmeier & Smith, 1978) to calculate R-factor.

$$R = \frac{1}{N}\sum_{i=1}^{N}\sum_{m=1}^{12} 1.735 \times 10^{\left(1.5\times\log_{10}\left(\frac{P_m^2}{P_i}\right)-0.08188\right)} \quad (2)$$

Where:

P_m = monthly rainfall of the month m

P_i = Annual rainfall of the year i

In evaluating erosivity in this study, the monthly rainfall spanning the years 2001 to 2022 was acquired from the Department of Hydrology and Meteorology (DHM). Five strategically located weather stations in and around the BRB: Hetauda NFI (0906), Makwanpurgadhi (0919), Hariharpurgadhi Valley (0910), and Godavari (1022) to collect data (Figure 4). There were many missing rainfall data, so it was statistically treated in MS Excel and filled using the Inverse Distance Method. Ultimately, the derived rainfall erosivity values are interpolated onto the watershed by applying Inverse Distance Weighted (IDW) techniques using ArcGIS.

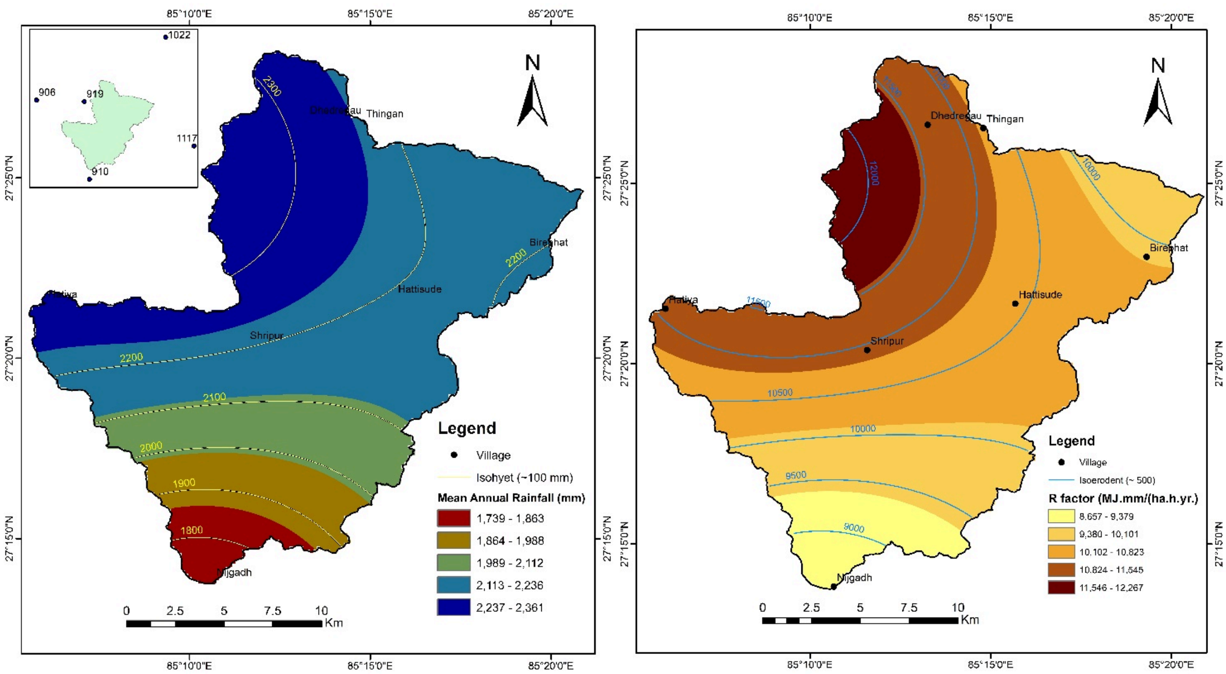

Fig. 4: Mean annual rainfall map with locations of the rainfall stations (Left) and annual erosivity map (Right) of the BRB

Soil Erodibility Factor (K)

The K-factor assesses soil erosion vulnerability, sediment transportability, and runoff under standard conditions. K-values are commonly derived from field measurements on runoff plots or indirectly using a standard monograph and empirical relations based on variables such as proportions of soil particles and organic matter, the diameter of the particle size, soil structure, and permeability (Bouyoucos, 1962; Denardin, 1990; Renard *et al.*, 1991; Wischmeier & Smith, 1978). The classification of soil types within the study area was conducted following the USDA textural classification system and the soil map of BRB was prepared through the fieldwork. The soil samples of about 54 localities were subjected to grain size analysis to classify the soil using the USDA textural soil classification system based on the proportion of sand, silt, and clay (Figure 5). Finally, a K-factor value is assigned to each soil type based on established value based on organic matter content (Schwab *et al.*, 1981). The National Soil Research Centre's soil database provided information on the average organic matter in the BRB. The US customary unit is converted into SI units ($t.h.MJ^{-1}.mm^{-1}$) using multiplier of 0.1317.

Topographic Factor (LS)

In the RUSLE framework, the *L* and *S* factors are used to reflect how terrain influences erosion processes. As described by Wischmeier and Smith (1978), "L is defined as the horizontal distance extending from the onset of overland flow to the juncture where the slope gradient diminishes to the extent where sediment deposition occurs, or where runoff becomes channelized." Broadly speaking, erosion exacerbates as L increases due to increased downhill runoff accumulation. Similar to this, erosion increases when S increases due to an increase in velocity. Eq. (3) from RUSLE (McCool *et al.*, 1989; Renard *et al.*, 1991) are used to determine L for the entire basin.

$$L = \left(\frac{\lambda}{22.13}\right)^m \tag{3}$$

Where:

λ = horizontal slope length (in m)

m = slope length exponent which depends on proportion of rill erosion to interrill erosion and calculated using Eq. (4).

$$m = \frac{F}{1+F} \tag{4}$$

F is determined for the soil that are moderately prone to both rill and interrill erosion using the Eq. (5).

$$F = \frac{sin\theta}{0.0896[3.0 \times sin\theta^{0.8} + 0.56]} \quad (5)$$

Where:

θ = the slope angle in degree.

The steepness factor (S) is calculated as the relative soil loss from a given slope to that from a 9% incline under similar conditions. The S Factor is calculated using Eq. (6) (McCool *et al.*, 1989; Renard *et al.*, 1991).

$$S = 10.8 \times sin\theta + 0.03, s \leq 9\%$$

$$S = 16.8 \times sin\theta - 0.50, s > 9\% \quad (6)$$

Where:

θ = the slope angle in degree ($1° = 0.0175^c$ in Arc GIS);

s = the slope gradient in percentage.

The L and S factors are derived from the Digital Elevation Model (DEM) (Hickey *et al.*, 1994; Van Remortel *et al.*, 2001) applying Eq. (3) and (6). Finally, LS factor is obtained after the multiplication of both the factors.

Cover Management Factor (C)

The C-factor measures the impact of land use and management practices on the soil's resistance to erosive forces of rain and runoff. The C-factor lies in between 0 and 1, where 0 represents completely impermeable surfaces such as pavement, and 1 signifies bare, tilled, and unprotected soil. Since Nepal doesn't have standard C factor values based on land uses, and measuring it across large areas isn't viable, an empirical approach was applied in this study. C- factor has been effectively correlated with Normalized Difference Vegetation Index (NDVI) in various scientific analyses (De Jong, 1994; Gutman & Ignatov, 1998; Van der Knijff *et al.*, 1999). To compute the C-factor, the empirical relation put forward by (Colman *et al.*, 2018; Durigon *et al.*, 2014) for the sub-tropical region characterized by intense rainfall, was used as in Eq. (7).

$$C = 0.1 \times \frac{-NDVI + 1}{2} \quad (7)$$

Where, NDVI was derived using the standard formula (Tucker, 1979) as in Eq. (8).

$$NDVI = \frac{NIR - Red}{NIR + Red} \quad (8)$$

For Sentinel-2 imagery, this corresponds to:

$$NDVI = \frac{Band8 - Band4}{Band8 + Band4}$$

All the cloud-free Sentinel-2 images from 2022 were processed through Google Earth Engine (GEE) to ensure high accuracy and eliminate cloud contamination. The median composite NDVI was computed using multiple images over the year because the median is less sensitive to outliers and cloud-related disturbances in the data.

Support Practice Factor (P)

The P-factor quantifies the soil erosion rate in various agricultural landscapes. Terracing, cropping, and contouring are a few examples of support practices that might help control erosion. The P-value ranges of 0 to 1, where 0 signifies a high degree erosion resistance due to human efforts. In Nepal, farming on hilly terrain involves building terraces that mimic contour farming, serving as a form of conservation agriculture. Therefore, contour farming was opted as an agricultural support practice in the study region, following the approach outlined in Shin (1999).

Validation

Since there is no sediment-discharge system installed in the BRB to monitor real-time soil loss, the model's evaluation and effectiveness were conducted using the Receiver Operating Characteristic (ROC) curve. It can measure the model performance quantitatively through the Area Under Curve (AUC). The ROC evaluates performance of the model by plotting its true positive rate against its false positive rate. A positive rate or sensitivity is the rate of correctly identifying soil erosion location. A false positive rate, or 1-specificity, is the proportion of low erosion locations which are incorrectly identified as erosion location. The required validation points were obtained from the detailed survey on erosion carried out in the BRB at the pre-selected points derived from satellite images and Google Earth. Furthermore, new erosion hotspots were also identified during fieldwork. All the obtained erosion validation points were collected from varying land use, soil types, and topography to reduce the bias in the validation of erosion severity. Finally, the curve was generated using ArcSDM Tool under the toolbox of ArcGIS with the input parameter of validation points and the RUSLE Model. Model's result were classified using rankings in Table 2 (Hosmer Jr, 2013; Lee, 2005).

Table 2: Accuracy Classification on the basis of AUC value Interval

AUC Value	Accuracy
0.90 – 1.00	Excellent
0.80 - 0.90	Good
0.70 - 0.80	Fair
0.60 - 0.70	Poor
0.50 - 0.60	Fail

Results

Rainfall Erosivity Factor (R)

Distinctive rainfall trends have been observed in BRB. Rainfall is highest from June to September, while remaining months of the year experiences much less rainfall. The southern section of BRB records 1739 mm of rainfall annually, while the northwest section receives 2361 mm (Figure 4). In the BRB, the average yearly precipitation is 2153 mm. The Rainfall Erosivity Map shows variations in erosivity values across the BRB, which provides information into the intensity of erosive forces in different regions. The rainfall erosivity value in the basin varies from 8657 to 12270 $MJ.mm.ha^{-1}.h^{-1}.yr^{-1}$. with an average erodent value of 10500 $MJ.mm.ha^{-1}.h^{-1}.yr^{-1}$. In the northern part of the BRB, Makwanpurgadhi records the highest erosivity value at 12,270 $MJ.mm.ha^{-1}.h^{-1}.yr^{-1}$.

On the other hand, the erosivity value in the Nijgadh region ranges from 8657 to 10100 $MJ.mm.ha^{-1}.h^{-1}.yr^{-1}$, the lower range in the basin. Shripur, Hattisude, and Thali villages and the northeastern part of the BRB demonstrate slightly higher erosivity values, ranging from 10,110 to 11,500 $MJ.mm.ha^{-1}.h^{-1}.yr^{-1}$. This indicates that the BRBs have an increasing trend of erosivity from southeast to northwest (Figure 4).

Soil Erodibility Factor (K)

BRB is characterized by all three types of soil based on genesis: residual, colluvial, and alluvial. The majority of the Siwalik zone consists of residual soil. Due to its fragile lithology, it is prone to weathering in the presence of rainfall. Alluvial soils are widely found in the central and southern flat lands of the BRB. Similarly, colluvial soils are identified at the basin's upper reaches, typically having steeper slopes.

Based on the USDA textural classification system, a soil map of the BRB is made after the investigation of the proportions of sand, silt, and clay. The BRB comprises three soil types: sandy loam, sand, and loamy sand. A major portion of the BRB is distributed by sand with parent material of sandstone, greywacke, and arkose. The villages, such as Shripur and Hattisude in the central belt, comprise loamy sand of fluvial origin. Similarly, the northernmost part of the BRB has loamy sand derived from the meta-sedimentary rock, such as quartzite and phyllite of the Lesser Himalaya. Following the National Soil Science Research Center Meta database on soil, the composition of the organic content varies from 2 to 3%. The mean spatial distribution of the organic matter content is equal to 2.

The erodibility value of the soil in the BRB is 0.0158 $t{\cdot}h{\cdot}MJ^{-1}{\cdot}mm^{-1}$ (Loamy Sand), 0.0211 $t{\cdot}h{\cdot}MJ^{-1}{\cdot}mm^{-1}$ (Sand), and 0.0355 $t{\cdot}h{\cdot}MJ^{-1}{\cdot}mm^{-1}$ (Sandy Loam).

Topographic Factor (LS)

Increased L-factor causes surface runoff to gradually accumulate in a downward direction, increasing soil erosion in that area. The increase in S value also encourages surface runoff velocity and soil erosion. These two factors determine the role of topography on erosion. With the aid of ALOS PALSAR DEM with a spatial resolution of 12.5m, F, and m values, the L-Factor has been determined using flow accumulation from the spatial analysis tool in ArcGIS. The f-value is essential in demarcating the depositional and erosional area. The f-value of BRB ranges from 0 to 3.1. The major depositional area falls within the flood plains and the river channels of the Bakiya River. The BRB shows m-values between 0 and 0.75, with a mean of 0.61.

The L-factor was determined on the basis of slope map generated from the DEM. Slopes within the BRB range from 0° to 76°which are classified into six classes (Figure 6). A very gentle slope (0°-5°) lies in the central belt, specially formed by the Bakiya River. The gentle slope (5°-10°) to moderate (10°-15°) falls on the periphery of the Major River and tributaries. The steep (15°-30°) to very steep slopes (>30°) are found in the hills of the northern and southern belts, which represent 57% of BRB. With this relation, a slope steepness map is prepared.

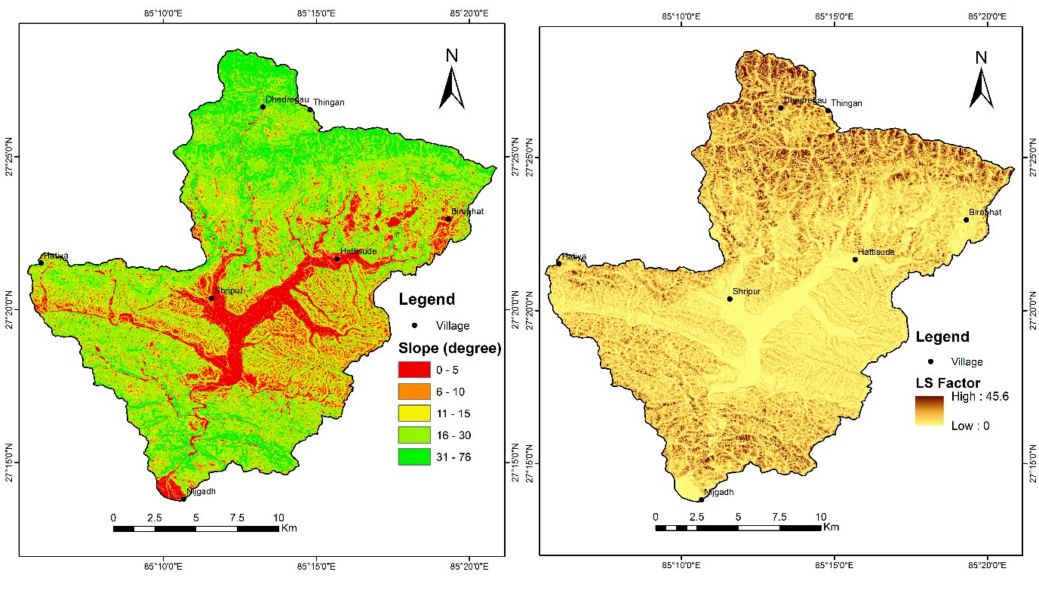

Fig. 6: Slope Map (Left) and LS-Factor Map (Right) of BRB

DOI: 10.3844/ajgsp.2025.1.18

The range of the LS-factor within BRB is 0 to 45. The steeper slopes in the northern and southern hills of the basin show the highest LS factor, while the lower values fall within the valley of the mainstream and its major tributaries.

The mean LS-factor is 11.88, which indicates that the spatial distribution of the maximum value is limited. Results signify that the steeper slopes in the northern boundary and in the southern belt play an influential role in the higher potential for soil loss. In contrast, regions within the valley and terraces of the river, with flat to gentle slopes and extended slope lengths, have a low potential for soil erosion.

Conservation Management Factor (C)

Vegetative cover, tillage practices, crop rotation, and mulching influence C-factor. NDVI values are standardized between -1 and +1, reflecting the degree of vegetation cover and health. The major river channels, water bodies, barren land, and ridges show less NDVI values, whereas the forest with abundant vegetation has higher NDVI (0.6 to 0.9). In the BRB, NDVI of the range -0.2 to 0 represent water bodies (Figure 7). The NDVI value ranges from 0.1 to 0.3, indicating rocks, sand, and barren land. Similarly, the value of 0.4 to 0.5 represents settlement with cultivation. Sparse vegetation and agricultural land are represented by 0.6 to 0.7 values. A value exceeding 0.7 represents a dense forest with vegetation in good health. Since the NDVI value is obtained from the time series of the whole year of 2022, it is possible to demarcate the NDVI value of the KTFT project, which is in the range of 0.1 to 0.4.

From the NDVI, the C-factor of BRB was obtained, and an inverse relation was illustrated (Figure 7). C-factor declines with increasing NDVI. The C-factor value varies from 0 to 0.05 (Figure 7). The barren land and water bodies show C-factor of 0.027 to 0.05. In contrast, the dense forest with healthy vegetation shows the range of 0 to 0.014 and reflects good cover to resist erosion from rainfall and helps reduce runoff and overland flow.

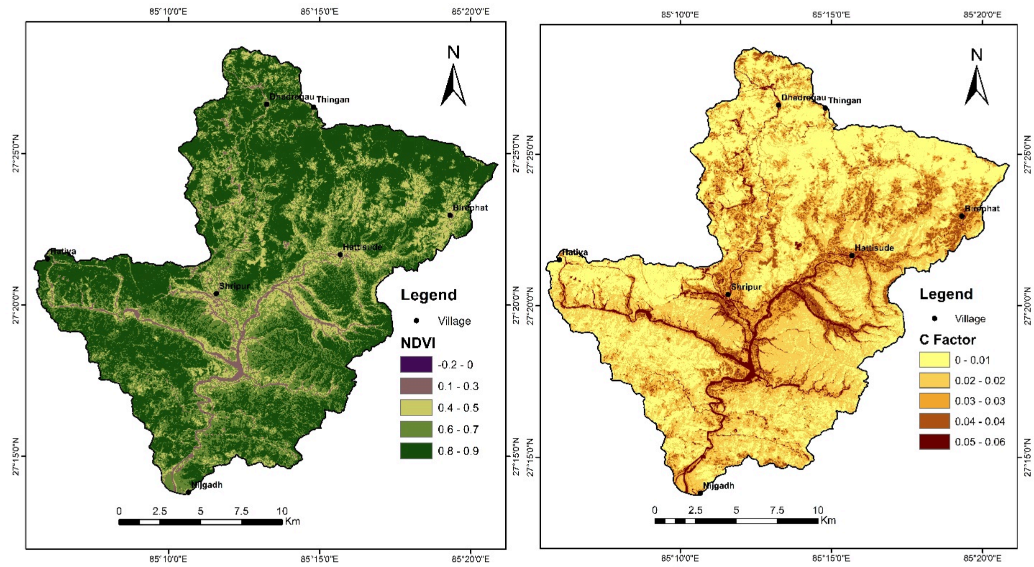

Fig. 7: NDVI (Left) and C-Factor (Right) Map of the BRB

Support Practice Factor (P)

The land cover type obtained from Sentinel-2's land cover produced by Microsoft, Esri, and Impact Observatory was used to determine the P-factor based on literature review. About 70.6% of the land in BRB is forested, whereas only 8% of the total area is used for agriculture, mostly for the cultivation of paddy fields and grain fields. The cultivation type in the study area is contouring type. No conservation practices based on LULC type have been observed during the field investigation. Hence, the P-factor is set to 1 for all the land cover types other than the agricultural land. In accordance with the cultivation method and slope, the value of the support practice element for agricultural land was assigned (Shin, 1999). The majority of the agricultural land shows a P-factor value of 0.55. (Figure 8).

Annual Soil Loss

The multiplication of aforementioned factors resulted in an annual soil erosion map of the BRB (Figure 9). The resulting map shows the soil loss annual range across the BRB from 0 to 729.65 t.ha-1.yr-1 with the average estimated at 41.82 t.ha-1.yr-1. Erosion intensity have been categorized into seven categories (Morgan *et al.*, 2005): Very Slight (<2 t.ha-1.yr-1), Slight (2-5 t.ha-1.yr-1), Moderate (5-10 t.ha-1.yr-1), High (10-50 t.ha-1.yr-1), Severe (50-100 t.ha-1.yr-1), Very severe (100-500 t.ha-1.yr-1), and catastrophic (>500 t.ha-1.yr-1) (Table 3).

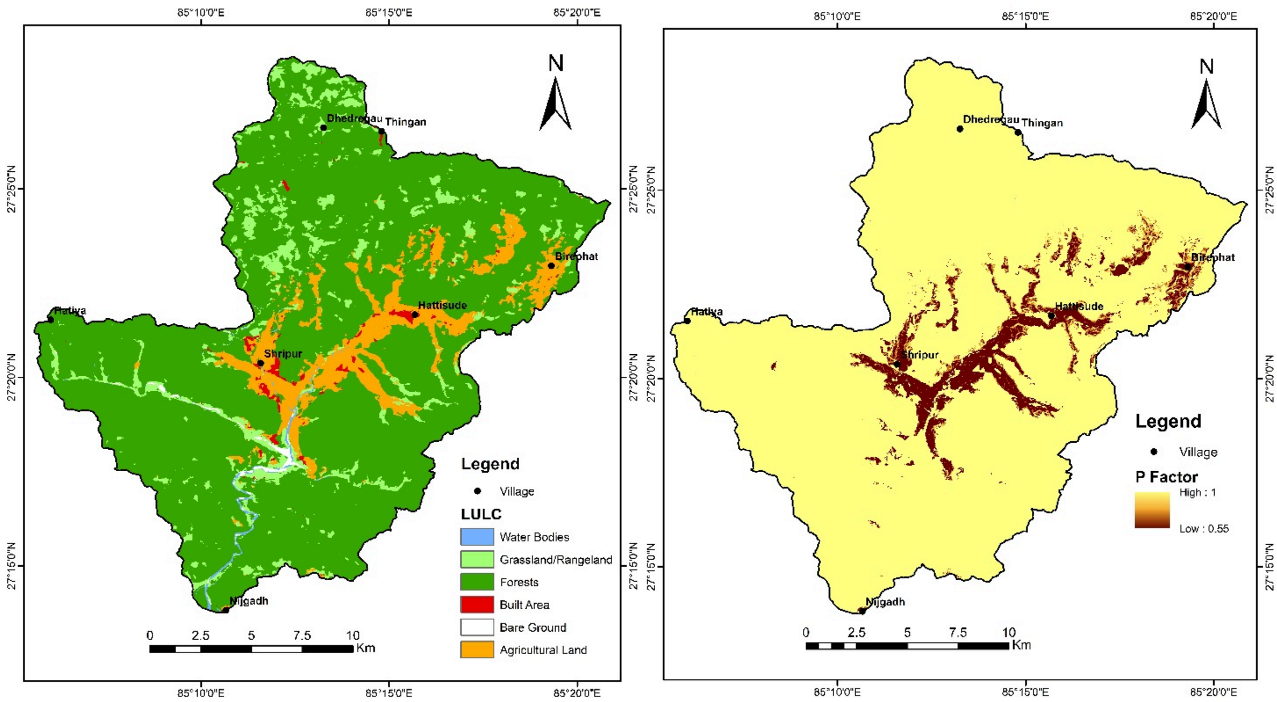

Fig. 8: LULC (Left) and P-Factor Map (Right) of the BRB

Table 3: Soil Erosion distribution in the BRB

Code	Class	Erosion Rate (t. ha-1. yr-1)	Area	
			Hectare	Percentage
1	Very Slight	<2	1538	5
2	Slight	2-5	1542	5
3	Moderate	5-10	1823	6
4	High	10-50	16766	53
5	Severe	50-100	8246	26
6	Very Severe	100-500	1928	6
7	Catastrophic	>500	2.4	0.007

The area with very slight erosion is limited, occupying only 5% of the total area (1538 hectares). Areas characterized by low-lying, flat terrains within the river valleys, such as those localities such as Shripur and Hattisude, along the Bakiya River and its major tributaries, exhibit minimal to very slight erosion. The southernmost part of the BRB, encompassing the Indo-genetic plain, experiences either negligible or no erosion at all. A similar proportion of the watershed (5%, or 1542 hectares) experiences slight erosion. Moderate erosion covers 6% of the watershed, with 1823 hectares falling under this category. Moderate types of erosion are observed on either side of the hill slope of rivers that flow across the wide alluvium plain at the central belt and northeastern belt.

The high erosion class constitutes most of the watershed area (53%, or 16766 hectares), signifying a portion of land vulnerable to erosion. Severe erosion accounts for 26% (8246 hectares) of the area, which is a significant soil degradation and requires urgent attention through conservation practices or land restoration efforts to avoid further erosion and long-term loss of land productivity. The very severe erosion class occupies only 6% (1928 hectares) of the watershed but indicates areas with extreme vulnerability. The E-W trending Churia hills of the southern belt and dissected hills at the upper reaches of the Simat River, are prominent in severe to very severe erosion. This causes extended soil loss that deeply affects soil fertility and, if untreated long-term, might lead to land degradation. Therefore, urgent interventions such as conservation practices or land restoration are needed to mitigate further erosion and prevent long-term land productivity loss.

Finally, catastrophic erosion affects a small part of the area (0.007% or 2.4 ha). Although the affected area is minimal, the erosion rate is alarming. Steep slopes, along with widespread grassland and rangeland use, make this location highly vulnerable to severe soil loss. Such a location is more prone to slope instability and debris flows and has a high carrying capacity of soil by surface runoff because of the high slope reaching up to 76°.

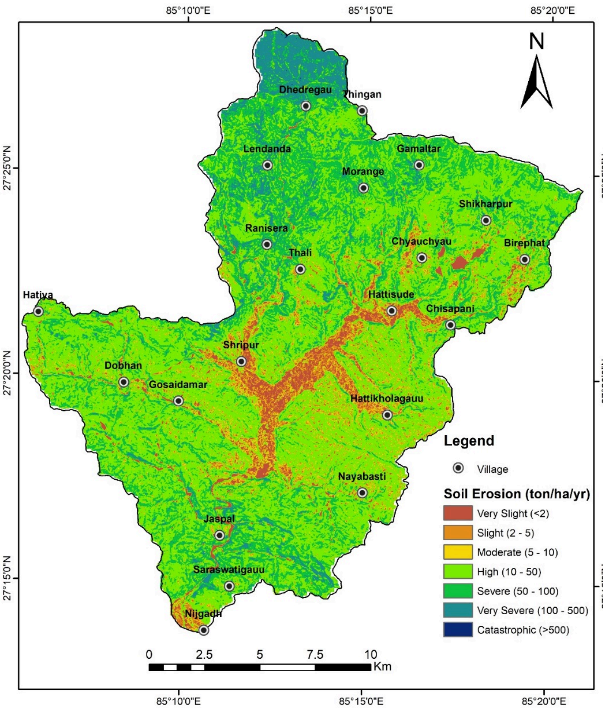

Fig. 9: Annual Soil Erosion Map of the BRB

Soil Loss on the Basis of Slope

Soil loss in BRB has been analyzed based on slope categories and erosion severity classes, which reflect a good correlation (Table 4). Very gentle slopes (0-5°) averaging erosion of 3.7 t.ha-1.yr-1 show low erosion severity classes. Their minimal slope gradient makes these areas relatively stable against erosion. The gentle slope shows moderate erosion with a mean of 15.11 t.ha-1.yr-1. Erosion rate starts to rise in areas with moderate slopes, which have an average soil loss of 27.56 $t{\cdot}ha^{-1}{\cdot}yr^{-1}$.

Steep slopes are the primary cause of severe and very severe erosion. Soil loss in these areas amounts to 50.69 $t{\cdot}ha^{-1}{\cdot}yr^{-1}$ on average. The steep gradient increases runoff abruptly and soil detachment, making areas more susceptible to erosion. Extreme soil (very severe to catastrophic) loss occurs on very steep slopes (>30°) in BRB. These areas are extremely fragile and require quick conservation actions to avoid further degradation.

Soil Erosion on the Basis of Land Use Scenarios

Land use and land cover play crucial role in the erosional process. Some land use, such as vegetation cover and grassland, acts as a shield against soil, whereas land use such as bare land accelerates erosion of the particular land. This study estimated the soil erosion scenarios on the basis of land use and land cover beside water bodies, which contribute less to the erosional process; they contribute to the transportation process. Table 5 presents a statistical summary of soil loss rates across different LULC categories.

Forested areas show a wide range, with the lowest soil loss recorded at 0.047 t. $ha^{-1}yr^{-1}$ and the highest at 729.65 $t.ha^{-1}yr^{-1}$, with a mean of 43.029 t. $ha^{-1}yr^{-1}$. Agricultural land has a range from no measurable soil loss (0 $t.ha^{-1}yr^{-1}$) to a maximum of 239 ton/ha/yr, with an average of 14.73 $t.ha^{-1}yr^{-1}$. The range of 0.042 to 327.038 $t.ha^{-1}yr^{-1}$ is seen in built-up areas where major localities are nestled, with 19.34 $t.ha^{-1}yr^{-1}$ on average. Bare ground areas, characterized by a lack of vegetation cover, range from 0 $t.ha^{-1}yr^{-1}$ to 263.64 $t.ha^{-1}yr^{-1}$, with an average of 12.55 $t.ha^{-1}yr^{-1}$. Bare ground can have a direct influence on rainfall and lead to erosion. Grasslands and rangelands vary from 0 $t.ha^{-1}yr^{-1}$ to 682.32 $t.ha^{-1}yr^{-1}$, with the highest average soil loss of 69.317 $t.ha^{-1}yr^{-1}$. This land use system is primarily found on the steeper slopes of BRB and has less vegetation.

Table 4: Soil Erosion based on the slope in the BRB

Class	Slope (°)	Area under each erosional class (Hectare)							Total Area		Erosion Rates (t. ha^{-1}. yr^{-1})		
		1	2	3	4	5	6	7	Hectare	%	Min	Max	Mean
Very Gentle	0-5	1496	1310	750	299	6	0.89	-	3861.89	12	0	242	3.7
Gentle	5-10	41	228	993	3115	45	4	-	4426	13	0	365	15.11
Moderate	10-15	6	16	60	4699	353	10	0.01	5144.01	16	0	551	27.56
Steep	15-30	2	3	10	8331	4954	652	0.01	13952.01	44	0	533	50.69
Very Steep	>30	0.14	0.07	0.07	291	2895	1266	2	4454.28	14	0	729.6	94.54

Table 5: Soil Erosion Based on LULC

LULC	Area under each erosion Class represented by code (hectare)							Total Area	Erosion Rate (tha^{-1}yr^{-1})		
	1	2	3	4	5	6	7		Minimum	Maximum	Mean
Forests	447	692	1133	14918	7318	1332	0.42	25840.42	0.047	239	43
Agricultural Land	781	681	404	874	220	24	-	2984	0	730	16
Bare Ground	57	11	22	27	6	3	-	126	0	596	14
Grassland/ Rangeland	165	104	187	826	667	543	2	2494	0.042	256	66.08
Built Area	33	45	60	91	19	8	-	256	0	264	18

DOI: 10.3844/ajgsp.2025.1.18

Model Performance and Validation

The erosion hotspots were identified in the field appraisal based on features and imprints such as exposed tree roots, crusting of the soil surface, vegetation cover type, development of splash pedestals, and the dimensions of rills and gullies. A total of 80 validation points (Figure 10) were identified to assess the model's performance using the ROC-AUC curve. The accuracy was achieved by comparing validation points with the simulated erosion raster map. From the ROC-AUC plot (Figure 11), the AUC value for the soil erosion model is 0.827, which can be converted into a percent success accuracy rate of 82.7%. Thus, the obtained AUC value falls under the "Good" accuracy class. Hence, Validation result quantitatively indicates that the RUSLE-based soil erosion estimation for the BRB offers satisfactory result.

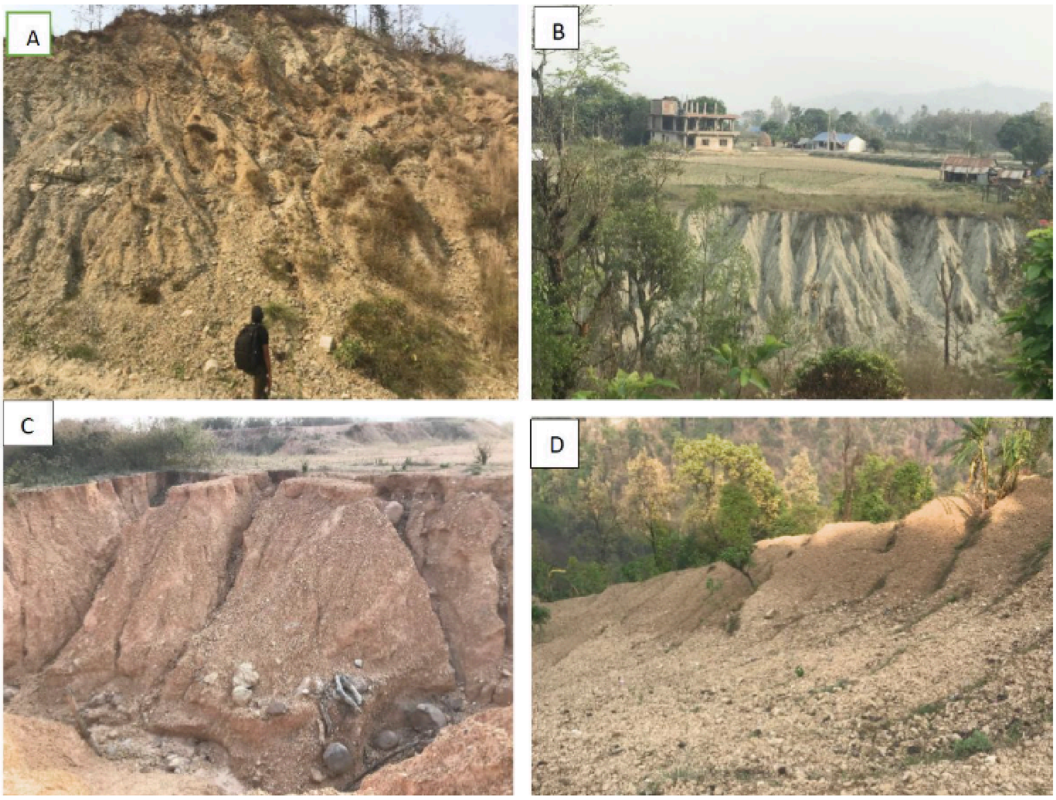

Fig. 10: Erosion hotspot area (A) high erosion with connected and continuous network of rills every 5-10 meters, (b) Severe erosion with continuous network of rills and gullies, less tree root exposure and bare soil in Shripur Village, (c) High Erosion with continuous rill formation with splash pedestals and soil mounds in the lateritic soil derived from the Pre-Siwalik rocks at Thali Village, and (D) High erosion potential terrace farming with no levees to prevent surface runoff in Lendanda area

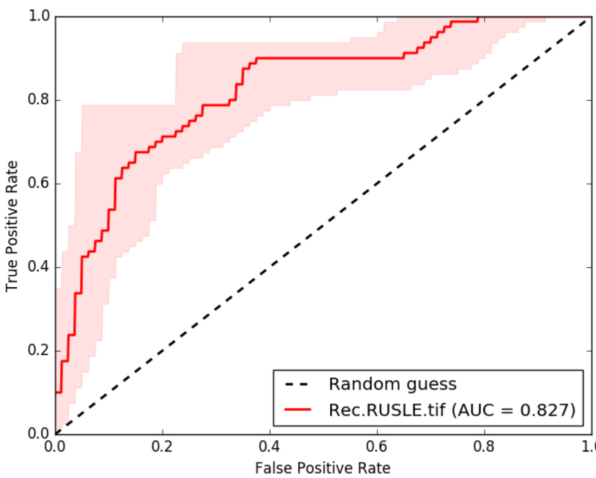

Fig. 11: ROC Plot and AUC for validation of Soil Erosion Model from RUSLE

Discussion

This research seeks to investigate the soil erosion of BRB, considering several causative factors that accelerate the erosion rate. The R-factor map shows how differences in rainfall intensity influence soil erosion potential throughout the basin. The BRB region demonstrates two distinct erosivity trends: i) a south to north increase of approximately 3000 $MJ.mm.ha^{-1}.h^{-1}.yr^{-1}$ and ii) and east to west rise of around 2000 $MJ.mm.ha^{-1}.h^{-1}.yr^{-1}$. The higher erosivity is confined to the Makwanpurgadhi area, which lies in the foothills of the adjacent Mahabharat range. This variation arises from orographic uplift especially on the south-facing Himalayan foothills where moist air collide and cause heavy rainfall (Bookhagen & Burbank, 2010; Shrestha *et al.*, 2019). These hills act as a physical barrier to such effects. In the Himalayas, the

DOI: 10.3844/ajgsp.2025.1.18

precipitation varies between ridge and valley within a short spatial extent (Andermann *et al.*, 2011; Barros *et al.*, 2004). BRB comprises erosivity ranges from 8657 to 12268 $MJ.mm.ha^{-1}.h^{-1}.yr^{-1}$, averaging 10500 $MJ.mm.ha^{-1}.h^{-1}.yr^{-1}$. The Global Rainfall Erosivity Database (GLoREDA) (Panagos *et al.*, 2022) estimated the global annual erosivity value, which also shows that the R-factor in BRB ranges between 8682 and 4779.08 $MJ.mm.ha^{-1}.h^{-1}.yr^{-1}$, with a mean value of 7149 $MJ.mm.ha^{-1}.h^{-1}.yr^{-1}$. This value suggests that the BRB falls in the class with the highest erosivity globally. Likewise, (Talchabhadel *et al.*, 2020b) estimated the mean annual erosivity of Nepal to be 9434.4 $MJ.mm.ha^{-1}.h^{-1}.yr^{-1}$ using sub-hourly rainfall data. This study suggests that the present study area has erosivity from 10000 to 15000 $MJ.mm.ha^{-1}.h^{-1}.yr^{-1}$. The R-factor in the Girwari watershed, which has similar physiographic and geological characteristics with BRB, was recorded between 10,569.41 and 10,441.65 $MJ.mm.ha^{-1}.h^{-1}.yr^{-1}$ (Tiruwa *et al.*, 2021).

The K-factor measures the resistant of a soil to erosion, based on its physical and chemical composition. BRB consists of three soil types, Sandy loam, Sand, and Loamy Sand, following the USDA textural classification system. The watershed is mainly dominated by Sand, which is primarily derived from the parent rock of the Siwalik region, namely, sandstone, silt, and mudstone. Likewise, Loamy Sand in the central belt of BRB is derived from the alluvial deposits of the Bakiya River. Meta-sedimentary rock weathering leads to Sandy Loam's formation in the northernmost section. Given the prevalence of gravel across the entire watershed, its presence within the soil matrix is a deterrent to soil detachment caused by rainfall. These gravel fragments can significantly impede water infiltration when integrated into soil profiles characterized by coarse textures such as sandy and loamy Sand. The soil is protected from impact of raindrop by the presence of gravel or rock fragments acting as a shield. These elements are typically resistant to displacement by rainwater in areas between rills, and they tend to stay on the soil surface, effectively functioning as a protective armor (Jennings & Jarrett, 1985). So, the rock fragments (>2mm) are excluded while estimating the K-factor (Renard *et al.*, 1991).

The interplay between L and S influences surface runoff accumulation and erosion. Examining the topographic factors helps define the role contributing to erosion. The majority of the topography in BRB comprises steep to very steep slopes (about 57% of the total area). This Figure accounts for high erosion susceptibility. The LS-factor in the high hills and the dissected valley are elevated, whereas they are low in the flat alluvial plains in the southern and central sections. The LS factor of the BRB progressively increases in the Northern Belt from the central alluvial plain to the northern tip. Meanwhile, in the southern belt, the LS-factor gradually increases towards the Churia Hills and decreases in the southern alluvium plain of the Indo-Gangetic plain.

The c-factor value determines the influence of the natural shield on rainfall. NDVI is an important indicator to identify the type of land use in a particular area. Nepal has no standard C-factor value based on LULC. So, NDVI is the most effective tool for determining the C-factor. NDVI in BRB shows a good vegetative cover. The C-factor between 0 and 0.05 in the BRB, which means that the basin has an appreciable volume of impermeable surfaces. This value suggests that the erosion potential regarding cover management is low. Despite majority of the area consists of forest, the Makawanpur District including BRB region is under high wild fire vulnerable zone (Mishra *et al.*, 2023). This assessment of fire in forest area during our field work in BRB reflects the deterioration of the cover management in that region. The P-factor determines the role of human intervention to erosion. During the field investigation, no control measures were taken by BRB for the conservation of soil. Consequently, all LULC types except agricultural land have a factor of 1. Agricultural land only holds 8% of the total land, and its contribution to holding soil from erosion is less in the basin. The contour farming method in BRB has a P-factor between 0.55 to 1 as per the slope gradient.

The synthesis of various factors culminates in preparing an annual soil loss map of the BRB. The annual average erosion averages 41.82 $t.ha^{-1}.yr^{-1}$ in the BRB, with minimum and maximum values of 0 and 729.65 $t.ha^{-1}.yr^{-1}$ respectively. The severity of erosion has been classified based on Morgan's field appraisal classification system, categorizing the basin into seven erosion classes. The results indicate that most areas fall under the high erosion class. Low erosion rates, comprising the Very Slight, Slight, and Moderate classes, account for 16% of the basin. Conversely, High, Severe, Very Severe, and Catastrophic erosion classes collectively cover a substantial area (85%), raising serious concerns regarding soil conservation.

Although the Catastrophic erosion class is confined to small patches at elevations between 2100m and 2200 m, it poses a significant hazard, including debris flows and sedimentation. These areas have been verified through remote sensing analysis and field investigations, revealing an extensive network of rills and gullies and evidence of substantial soil mass removal. Large deposits of sediments, including boulders, cobbles, pebbles, and fine particles, observed downstream of the Simat River at Dhedregaun provide strong evidence of catastrophic erosion. In Nepal, the erosion intensity of such a class has been reported in the northern region of Rapti River Basin (Patel *et al.*, 2024). Similar extreme erosion patterns have also been reported in countries like Pakistan and Afghanistan (Bhatti *et al.*, 2021), India (Raj *et al.*, 2024), and Tianshan Mountains, China (Wei *et al.*, 2024).

Rainfall intensity, topographic features, and land use patterns influence rate of erosion varied spatially within the BRB. Erosion rates increase from the plains and river valleys toward adjacent ridges. A comparative analysis across the BRB reveals higher erosion rates in the northern section compared to southern section, primarily of increased erosivity in the northern region. Topography plays a crucial role in determining erosion severity. Very gentle to gentle slopes are associated with Very Slight to Slight erosion classes, whereas steep to very steep slopes exhibit higher erosion rates, falling within the High, Severe, Very Severe, and Catastrophic erosion classes.

Land use significantly influences soil erosion dynamics across the BRB. Grasslands and rangelands in the basin's upper reaches have greater rate of erosion, averaging 68.08 t.ha-1.yr-1. This rapid erosion rate is due to the areas' high rainfall, lack of vegetation coverage, and increased slope gradient. Forested areas have an annual average soil erosion rate of 43 t.ha-1.yr-1, which varies based on the forest type and size. Bare terrain has a lower erosion rate of 14 t.ha-1.yr-1due to its location on gentle slopes. Agricultural land also demonstrates relatively low erosion rates due to farming practices such as terracing and contouring, with an erosion rate of 14 t.ha-1.yr-1 annually. Similarly, built-up areas exhibit a moderate erosion rate of 18 t.ha-1.yr-1.

Several studies have been undertaken in river basins and watersheds in the Nepal Himalayas using the RUSLE Model and GIS. Similarly, in Andhi Khola and Tinau Khola of Western Nepal, both identical to the present study area in terms of physiography and geology (Joshi *et al.*, 2023), estimated mean erosion rates of 41.4 $t.ha^{-1}.yr^{-1}$ and 24.1 $t.ha^{-1}.yr^{-1}$, where an experimental plot supported the output of the model. The result of Andhi Khola is similar to the present study, whereas there is a low erosion rate in Tinau Khola because it has a small area, and the majority of the area lies on a gentle slope. In the Aringale Khola area of Salyan district, part of middle mountains and Siwalik of Western Nepal, erosion rates is in between 0.03 and 100.3 $t.ha^{-1}.yr^{-1}$ (Chalise *et al.*, 2018). Compared to the present study, the low value is due to less erosivity value (365-435) despite having similar soil erodibility (0.55-0.006) and geology.

Likewise, the average erosion rate in the Khajuri watershed, Eastern Nepal was 64 $t.ha^{-1}.yr^{-1}$ using field measurement (Ghimire *et al.*, 2013). This higher value was accounted for by measuring erosion from landslides and stream bank erosion. (Tiruwa *et al.*, 2021) reported erosion between less than 2 and 190 $t.ha^{-1}.yr^{-1}$ in the Girwari River watershed in the Siwalik Hills of Nawalparasi, where steep terrain and inadequate conservation practices exacerbate erosion. Their study found that hilly forest regions had a maximum soil loss of 189.26 $t.ha^{-1}.yr^{-1}$. Additionally, (Talchabhadel *et al.*, 2020a) concluded 8.1 $t.ha^{-1}.yr^{-1}$ of soil loss in the West Rapti River Basin annually, which is expected to grow by 10% in the future. The study found that rainfall erosivity and slope gradient had significant effects on the results.

It is a crucial step to perform the accuracy of the model and its reliability to assess soil erosion in different watersheds. The accuracy rate of estimates using the ROC-AUC validation method is 82.7 %, classifying it as good accuracy. The validation result of the BRB using the ROC-AUC curve is consistent with results from West Bengal, India (Biswas & Giri, 2023), Central Highlands, Sri Lanka (93%), Peshawar Basin, Pakistan (81.9%) (Sarwar *et al.*, 2024), Bangladesh (94%) (Islam *et al.*, 2024), West Kameng Watershed, Eastern Himalaya (84.9%) (Das *et al.*, 2020). Thus, the reliability in different region other than the present study context, has proved RUSLE an essential tool for policy maker to asses erosion rate in an ungauged basin of Nepal. Furthermore, the study in Tinau Khola and Andhi Khola of western Nepal reported that RUSLE and erosion plot provides similar result (Joshi *et al.*, 2023).

Soil loss tolerance (T) is the maximum amount of soil erosion each year while maintaining long-term sustainable crop productivity (McCormack *et al.*, 1982). In general, natural geological processes in undisturbed places cause soil erosion, which is considered normal and acceptable (El-Swaify *et al.*, 1982; Smith & Stamey, 1965). Several aspects are considered while estimating the T value, such as the natural rate of soil formation or deposition through weathering, the influence of soil loss on productivity, and how eroded sediments affect water quality and adjacent surroundings (Mannering, 1981). The maximum permissible T-value of 11.2 $t.ha^{-1}.yr^{-1}$ is considered worldwide (Mandal *et al.*, 2006; Wischmeier & Smith, 1978) has estimated 2.2 to 12.5 $t.ha^{-1}.yr^{-1}$ in NW Himalaya. Likewise, (Bhattacharyya *et al.*, 2008) estimated T values ranging between 2.5 to 12.5 $t.ha^{-1}.yr^{-1}$ based on different soil indicators in Shivalik-Himalaya. However, there is no study on soil loss tolerance of the soil in Nepal Himalaya considering all the parameters. It is considered 25 $t.ha^{-1}.yr^{-1}$ of soil erosion tolerable in mountainous regions like Nepal Himalaya (Morgan, 2009; Shrestha, 1997). With this threshold value of soil erosion practice in Nepal, BRB is critical in terms of erosion, with 65% of its area (about 21076 hectares) needing immediate conservation policies.

Conclusion

Using RUSLE model with geospatial technology, this study quantitatively estimated and mapped erosion rates. Primary and secondary data available in Nepal were used to obtain required input layers. The findings align well with other studies conducted at both national and local levels.

The highest erosion rates were observed in the northern regions, particularly in the upper reaches marked by the Mahabharat Hills and in the southern hills dominated by the Churia Hills. In contrast, the central flat alluvial plains and the southern territories of the basin showed the lowest erosion rates. Furthermore, soil erosion affects over 65% of the BRB's total area. Erosion rates are highest in grasslands, rangelands, and certain forested zones, whereas urban areas, farmlands, and barren landscapes has minimal soil erosion.

The accuracy of the model was performed using the ROC-AUC Curves. The model's performance is found to have "Good accuracy." This validation provides the reliability of the estimated outcomes of erosion and proves suitability of RUSLE model in similar ungauged basins.

The assessment of erosion in BRB is supported by primary and secondary, secondary data, which provides a useful resource for tackling land degradation at federal, provincial, and local levels in Nepal. This study provides important information for policymakers and stakeholders to effectively address soil erosion and land management challenges.

Recommendations

In order to make RUSLE and GIS technology effective in conducting soil erosion hazard assessment in Nepal Himalaya, empirical relations and methodology for all the required factors need to be established for a better understanding of soil loss in different river basins. The soil loss tolerance limit should be assigned per the soil erosion scenario in Nepal using all the parameters of the soil available in Nepal. Based on the findings of this study from the RUSLE Model, the following conservation strategies are recommended to mitigate soil erosion in BRB.

Agronomical Measures: A contour Farming system should be practiced in cultivated lands on moderate to steep slopes to minimize soil erosion and promote soil stability. The agroforestry system should be implemented by introducing tree species such as Dalbergia sisso and Acacia catechu with the crop planta. It helps in improving soil retention and reduces surface runoff. In the rangeland and exposed cultivated lands, cover cropping and mulching techniques can be effective measures to protect soil from rainfall and increase moisture retention. Similarly, crop rotation and intercropping with legumes such as peas and beans also help in improving soil structure and organic matter content.

Mechanical Measures: Terracing and contour bunding should be implemented in the high erosion zones, such as the Mahabharat and Churia ranges. This will help reduce runoff and soil detachment in agricultural land. In the high erosion zones, check dams and gully plugs should be constructed for sediment traps and to stop surface runoff. Gabion walls and rock barriers along river banks and hill slopes should be installed to reduce the impact of bank erosion and slope instability. Retention basins and silt traps near the foothills should be used to minimize the transportation of sediments further downstream. Additionally, bioengineering techniques such as vetiver grass and bamboo plantations should be applied to reduce erosion and stabilize soil in hilly terrane.

Constructing riparian buffer zones and reinforcing embankments using natural and engineered materials will help protect river banks and control floods. This helps reduce erosion during peak monsoon flows in rivers.

Rainwater harvesting structures such as farm ponds and retention basins, spring water storage tanks in upper reaches of the BRB, check dams, and percolation ponds can help reduce soil erosion due to slow runoff.

Conservation policies should be enforced to regulate deforestation, wildfire, unplanned road networks, and encroachment of soil erosion zones. Local communities, farmers, and landowners should be encouraged, trained, and taught on sustainable land management.

Regular monitoring of soil erosion using remote sensing techniques and field surveys, along with the real-time rainfall runoff and sediment load in the river, need to be installed and monitored. Soil erosion modeling such as RUSLE needs to be updated continuously with field data to improve the accuracy of the assessment of erosion in the basin.

Acknowledgment

The author extends sincere gratitude to Roshan Saud, Sudeep Bista and Samir Ghimire for their valuable assistance in data extraction and technical support. This research was conducted under the academic affiliation of the Central Department of Geology, Tribhuvan University, Kathmandu, and the author acknowledges the institutional support provided.

The author also acknowledges the Department of Geology and the Department of Hydrology and Meteorology, Government of Nepal, for their indirect support through data accessibility. Finally, thanks are due to colleagues and peers for their constructive feedback during the preparation of this manuscript.

Funding Information

This research received no external funding. All costs associated with this study were covered by the author’s personal resources.

Author’s Contributions

Sujan Bista: Participated in research design and methodology, fieldwork, lab analysis, map preparation data acquisition, validation, and interpretation, and manuscript preparation and revision.

Naresh Kazi Tamrakar: Contributed to research planning, and review and revised the manuscript.

Kishor Rimal: Participated in field work, map preparation, and lab work.

Arju Bhattarai: Participated in field work and data acquisition and validation.

Ethics

All the authors affirm that this study was conducted in accordance with ethical principle. Data were not fabricated, manipulated, or misrepresented. All the authors contributed significantly and approved the final manuscript.

References

Andermann, C., Bonnet, S., Crave, A., Davy, P., Longuevergne, L., & Gloaguen, R. (2012). Sediment transfer and the hydrological cycle of Himalayan rivers in Nepal. *Comptes Rendus. Géoscience*, *344*(11–12), 627–635. https://doi.org/10.1016/j.crte.2012.10.009

Andermann, C., Bonnet, S., & Gloaguen, R. (2011). Evaluation of precipitation data sets along the Himalayan front. *Geochemistry, Geophysics, Geosystems*, *12*(7), n/a-n/a. https://doi.org/10.1029/2011gc003513

Angima, S. D., Stott, D. E., O'Neill, M. K., Ong, C. K., & Weesies, G. A. (2003). Soil erosion prediction using RUSLE for central Kenyan highland conditions. *Agriculture, Ecosystems & Environment*, *97*(1–3), 295–308. https://doi.org/10.1016/s0167-8809(03)00011-2

Arnoldus, H. (1977). *Methodology used to determine the maximum potential average annual soil loss due to sheet and rill erosion in Morocco*.

Ban, J. K., Yu, I., & Jeong, S. (2016). Estimation of Soil Erosion Using RUSLE Model and GIS Techniques for Conservation Planning from Kulekhani Reservoir Catchment, Nepal. *Journal of Korean Society of Hazard Mitigation*, *16*(3), 323–330. https://doi.org/10.9798/kosham.2016.16.3.323

Barros, A. P., Kim, G., Williams, E., & Nesbitt, S. W. (2004). Probing orographic controls in the Himalayas during the monsoon using satellite imagery. *Natural Hazards and Earth System Sciences*, *4*(1), 29–51. https://doi.org/10.5194/nhess-4-29-2004

Batista, P. V. G., Davies, J., Silva, M. L. N., & Quinton, J. N. (2019). On the evaluation of soil erosion models: Are we doing enough? *Earth-Science Reviews*, *197*, 102898. https://doi.org/10.1016/j.earscirev.2019.102898

Bhandari, B. P., & Dhakal, S. (2019). Evolutional Characteristics of Debris Flow in the Siwalik Hills of Nepal. *International Journal of Geosciences*, *10*(12), 1049–1067. https://doi.org/10.4236/ijg.2019.1012060

Bhattacharyya, P., Bhatt, V. K., & Mandal, D. (2008). Soil loss tolerance limits for planning of soil conservation measures in Shivalik–Himalayan region of India. *CATENA*, *73*(1), 117–124. https://doi.org/10.1016/j.catena.2007.10.001

Bhatti, M. T., Ashraf, M., & Anwar, A. A. (2021). Soil Erosion and Sediment Load Management Strategies for Sustainable Irrigation in Arid Regions. *Sustainability*, *13*(6), 3547. https://doi.org/10.3390/su13063547

Biswas, J., & Giri, B. (2023). RUSLE and AHP based soil erosion risk mapping for Jalpaiguri district of West Bengal, India. *Proceedings of the Indian National Science Academy*, *89*(4), 869–883. https://doi.org/10.1007/s43538-023-00197-3

Bohlinger, P., & Sorteberg, A. (2018). A comprehensive view on trends in extreme precipitation in Nepal and their spatial distribution. *International Journal of Climatology*, *38*(4), 1833–1845. https://doi.org/10.1002/joc.5299

Bonilla, C. A., & Vidal, K. L. (2011). Rainfall erosivity in Central Chile. *Journal of Hydrology*, *410*(1–2), 126–133. https://doi.org/10.1016/j.jhydrol.2011.09.022

Bookhagen, B., & Burbank, D. W. (2010). Toward a complete Himalayan hydrological budget: Spatiotemporal distribution of snowmelt and rainfall and their impact on river discharge. *Journal of Geophysical Research: Earth Surface*, *115*(F3). https://doi.org/10.1029/2009jf001426

Bouyoucos, G. J. (1962). Hydrometer Method Improved for Making Particle Size Analyses of Soils[1]*Agronomy Journal*, *54*(5), 464–465. https://doi.org/10.2134/agronj1962.00021962005400050028x

Chalise, D., Kumar, L., Shriwastav, C. P., & Lamichhane, S. (2018). Spatial assessment of soil erosion in a hilly watershed of Western Nepal. *Environmental Earth Sciences*, *77*(19), 1–11. https://doi.org/10.1007/s12665-018-7842-3

Cook, H. L. (1937). The Nature and Controlling Variables of the Water Erosion Process. *Soil Science Society of America Journal*, *1*(C), 487–494. https://doi.org/10.2136/sssaj1937.03615995000100000085x

Dahal, R., Hasegawa, S., Yamanaka, M., Bhandary, N., & Yatabe, R. (2010). Statistical and deterministic landslide hazard assessment in the Himalayas of Nepal. *IAEG 2010 Conference, Geologically Active*, 496–510. https://doi.org/10.1016/j.geomorph.2008.05.041

Das, B., Bordoloi, R., Thungon, L. T., Paul, A., Pandey, P. K., Mishra, M., & Tripathi, O. P. (2020). An integrated approach of GIS, RUSLE and AHP to model soil erosion in West Kameng watershed, Arunachal Pradesh. *Journal of Earth System Science*, *129*(1), 1–18. https://doi.org/10.1007/s12040-020-1356-6

De Jong, S. M. (1994). Derivation of vegetative variables from a landsat tm image for modelling soil erosion. *Earth Surface Processes and Landforms*, *19*(2), 165–178. https://doi.org/10.1002/esp.3290190207

Denardin, J. E. (1990). *Erodibilidade do solo estimada por meio de parâmetros físicos e químicos Universidade de São Paulo*. https://doi.org/10.11606/T.11.1990.tde-20230818-145355

Devkota, D. C., & Bhattarai, T. N. (2011). Impact of climate change and possible strategic programs for building climate resilient communities in Nepal. *Journal of Nepal Geological Society*, *43*, 219–224. https://doi.org/10.3126/jngs.v43i0.25617

Dhital, M. R. (2015). *Geology of the Nepal Himalaya: regional perspective of the classic collided orogen*. https://doi.org/10.1007/978-3-319-02496-7

DMG (2002). Geological Map of Petroleum Exploration Block-7 Malangawa. *Kathmandu, Petroleum Exploration Project, Department of Mines and Geology.*

Duncan, C. C., Klein, A. J., Masek, J. G., & Isacks, B. L. (1998). Comparison of Late Pleistocene and Modern Glacier Extents in Central Nepal Based on Digital Elevation Data and Satellite Imagery. *Quaternary Research*, *49*(3), 241–254. https://doi.org/10.1006/qres.1998.1958

Durigon, V. L., Carvalho, D. F., Antunes, M. A. H., Oliveira, P. T. S., & Fernandes, M. M. (2014). NDVI time series for monitoring RUSLE cover management factor in a tropical watershed. *International Journal of Remote Sensing*, *35*(2), 441–453. https://doi.org/10.1080/01431161.2013.871081

El-Swaify, S. A., Dangler, E. W., & Armstrong, C. L. (1982). *Soil erosion by water in the tropics*.

Galay, V. J. (1987). *Erosion and sedimentation in the Nepal Himalaya: an assessment of river processes*.

Ghimire, M., & Timalsina, N. (2020). Landslide Distribution and Processes in the Hills of Central Nepal: Geomorphic and Statistical Approach to Susceptibility Assessment. *Journal of Geoscience and Environment Protection*, *08*(12), 276–302. https://doi.org/10.4236/gep.2020.812017

Ghimire, S., Higaki, D., & Bhattarai, T. (2013). Estimation of Soil Erosion Rates and Eroded Sediment in a Degraded Catchment of the Siwalik Hills, Nepal. *Land*, *2*(3), 370–391. https://doi.org/10.3390/land2030370

Gitas, I. Z., Douros, K., Minakou, C., Silleos, G. N., & Karydas, C. G. (2009). Multi-temporal soil erosion risk assessment in N. Chalkidiki using a modified USLE raster model. *EARSel Eproceedings*, *8*(1), 40–52.

Gutman, G., & Ignatov, A. (1998). The derivation of the green vegetation fraction from NOAA/AVHRR data for use in numerical weather prediction models. *International Journal of Remote Sensing*, *19*(8), 1533–1543. https://doi.org/10.1080/014311698215333

Hickey, R., Smith, A., & Jankowski, P. (1994). Slope length calculations from a DEM within ARC/INFO grid. *Computers, Environment and Urban Systems*, *18*(5), 365–380. https://doi.org/10.1016/0198-9715(94)90017-5

Hosmer Jr, D. (2013). *Model-building strategies and methods for logistic regression*. 89–151. https://doi.org/10.1002/9781118548387.ch4

Islam, Md. R., Imran, H. M., Islam, Md. R., & Saha, G. C. (2024). A RUSLE-based comprehensive strategy to assess soil erosion in a riverine country, Bangladesh. *Environmental Earth Sciences*, *83*(6). https://doi.org/10.1007/s12665-024-11455-y

Jennings, G. D., & Jarrett, A. R. (1985). Laboratory Evaluation of Mulches in Reducing Erosion. *Transactions of the ASAE*, *28*(5), 1466–1470. https://doi.org/10.13031/2013.32461

Joshi, P., Adhikari, R., Bhandari, R., Shrestha, B., Shrestha, N., Chhetri, S., Sharma, S., & Routh, J. (2023). Himalayan watersheds in Nepal record high soil erosion rates estimated using the RUSLE model and experimental erosion plots. *Heliyon*, *9*(5), e15800. https://doi.org/10.1016/j.heliyon.2023.e15800

Kizaki, K. (1994). *An outline of the Himalayan upheaval: A case study of the Nepal Himalayas*.

Koirala, P., Thakuri, S., Joshi, S., & Chauhan, R. (2019). Estimation of Soil Erosion in Nepal Using a RUSLE Modeling and Geospatial Tool. *Geosciences*, *9*(4), 147. https://doi.org/10.3390/geosciences9040147

Lee, S. (2005). Application of logistic regression model and its validation for landslide susceptibility mapping using GIS and remote sensing data. *International Journal of Remote Sensing*, *26*(7), 1477–1491. https://doi.org/10.1080/01431160412331331012

Li, X., & Ye, X. (2018). Variability of Rainfall Erosivity and Erosivity Density in the Ganjiang River Catchment, China: Characteristics and Influences of Climate Change. *Atmosphere*, *9*(2), 48. https://doi.org/10.3390/atmos9020048

Lu, D., Li, G., Valladares, G. S., & Batistella, M. (2004). Mapping soil erosion risk in Rondônia, Brazilian Amazonia: using RUSLE, remote sensing and GIS. *Land Degradation & Development*, *15*(5), 499–512. https://doi.org/10.1002/ldr.634

Mannering, J. (1981). The use of soil loss tolerances as a strategy for soil conservation. *Soil Conservation: Problems and Prospects*, 337–349.

McCool, D. K., Foster, G. R., Mutchler, C. K., & Meyer, L. D. (1989). Revised Slope Length Factor for the Universal Soil Loss Equation. *Transactions of the ASAE*, *32*(5), 1571–1576. https://doi.org/10.13031/2013.31192

McCormack, D. E., Young, K. K., & Kimberlin, L. W. (2015). *Current Criteria for Determining Soil Loss Tolerance*. 95–111. https://doi.org/10.2134/asaspecpub45.c9

Millward, A. A., & Mersey, J. E. (1999). Adapting the RUSLE to model soil erosion potential in a mountainous tropical watershed. *CATENA*, *38*(2), 109–129. https://doi.org/10.1016/s0341-8162(99)00067-3

Mishra, B., Panthi, S., Poudel, S., & Ghimire, B. R. (2023). Forest fire pattern and vulnerability mapping using deep learning in Nepal. *Fire Ecology*, *19*(1). https://doi.org/10.1186/s42408-022-00162-3

Morgan, R., Hann, M., Shilston, D., Mirtskhoulava, T. E., Nadirashvili, V., Gasca, A., Clarke, J., & Sweeney, M. (2005). Use of terrain analysis as a basis for erosion risk assessment along pipeline rights-of-way: a case study from Georgia. *International conference on: Terrain and geohazard challenges facing onshore oil and gas pipelines*. https://doi.org/10.1680/tagcfooagp.32781

Morris, G. L., & Fan, J. (1998). *Reservoir sedimentation handbook : design and management of dams, reservoirs, and watersheds for sustainable use*.

Nearing, M. A. (2013). Soil erosion and conservation. *Environmental Modelling: Finding Simplicity in Complexity*, 365–378.

Olen, S. M., Bookhagen, B., Hoffmann, B., Sachse, D., Adhikari, D. P., & Strecker, M. R. (2015). Understanding erosion rates in the Himalayan orogen: A case study from the Arun Valley. *Journal of Geophysical Research: Earth Surface*, *120*(10), 2080–2102. https://doi.org/10.1002/2014jf003410

Panagos, P., Van Liedekerke, M., Borrelli, P., Köninger, J., Ballabio, C., Orgiazzi, A., Lugato, E., Liakos, L., Hervas, J., Jones, A., & Montanarella, L. (2022). European Soil Data Centre 2.0: Soil data and knowledge in support of the EU policies. *European Journal of Soil Science*, *73*(6), e13315. https://doi.org/10.1111/ejss.13315

Patel, A., Singh, M. M., Bhatt, S. C., de Oliveira-Júnior, J. F., Singh, S. K., Rathore, V. K. S., Sahu, S. K., & Sachan, H. (2024). Assessment of soil loss from a Trans-National Rapti River Basin using empirical and InVEST-based models. *Geomatica*, *76*(2), 100016. https://doi.org/10.1016/j.geomat.2024.100016

Pokhrel, A., Khanal, N., Khadananda Dulal, K. D., Rishi Rijal, R. R., Salikram Sigdel, S. S., Khanal, B., Yadav Subedi, Y. S., Chitra Acharya, C. A., Dhruba Thapa, D. T., & Bipin Acharya, B. A. (2013). *Lal Bakaiya Watershed, Nepal: challenges and opportunities in flash flood risk management*.

Prasannakumar, V., Vijith, H., Geetha, N., & Shiny, R. (2011). Regional Scale Erosion Assessment of a Sub-tropical Highland Segment in the Western Ghats of Kerala, South India. *Water Resources Management*, *25*(14), 3715–3727. https://doi.org/10.1007/s11269-011-9878-y

Raj, R., Saharia, M., & Chakma, S. (2024). Geospatial modeling and mapping of soil erosion in India. *CATENA*, *240*, 107996. https://doi.org/10.1016/j.catena.2024.107996

Renard, K. G., Foster, G. R., Weesies, G. A., & Porter, J. P. (1991). RUSLE: Revised universal soil loss equation. *Journal of Soil and Water Conservation*, *46*(1), 30–33. https://doi.org/10.1080/00224561.1991.12456571

Sarwar, A., Ali, M., Israr, M., Gulzar, S., Khan, M. I., Ali, M. A. S., Majid, A., & Rukh, S. (2024). Mapping annual soil loss in the southeast of Peshawar basin, Pakistan, using RUSLE model with geospatial approach. *Geology, Ecology, and Landscapes*, 1–12. https://doi.org/10.1080/24749508.2024.2373493

Schwab, G. O., Frevert, R. K., Edminster, T. W., & Barnes, K. K. (1955). Soil and Water Conservation Engineering. *Soil Science Society of America Journal*, *19*(4), 509–509. https://doi.org/10.2136/sssaj1955.03615995001900040033x

Sholagberu, A., Ul Mustafa, M., Wan Yusof, K., & Hashim Ahmad , M. (2016). Evaluation of Rainfall-Runoff Erosivity Factor for Cameron Highland, Pahang, Malaysia. *Journal of Ecological Engineering*, *17*(3), 1–8. https://doi.org/10.12911/22998993/63338

Shrestha, D. P. (1997). Assessment of soil erosion in the Nepalese Himalaya: a case study in Likhu Khola Valley, Middle Mountain Region. *Land Husbandry*, *2*(1), 59–80.

Shrestha, M. L. (2000). Interannual variation of summer monsoon rainfall over Nepal and its relation to Southern Oscillation Index. *Meteorology and Atmospheric Physics*, *75*(1–2), 21–28. https://doi.org/10.1007/s007030070012

Shrestha, M., Tamrakar, N., & Miyazaki, T. (2008). Morphometry and Sediment Dynamics of the Churiya River Area, Siwalik Range in Nepal. *Boletin de Geología*, *30*, 35–48.

Shrestha, S., Yao, T., & Adhikari, T. R. (2019). Analysis of rainfall trends of two complex mountain river basins on the southern slopes of the Central Himalayas. *Analysis of Rainfall Trends of Two Complex Mountain River Basins on the Southern Slopes of the Central Himalayas*, *215*, 99–115. https://doi.org/10.1016/j.atmosres.2018.08.027

Smith, R. M., & Stamey, W. L. (1965). Determining the Range of Tolerable Erosion. In *Soil Science* (Vol. 100, Issue 6, pp. 414–424). https://doi.org/10.1097/00010694-196512000-00007

Strahler, A. N. (1952). Hypsometric (Area-altitude) Analysis of Erosional Topography. In *Geological Society of America Bulletin* (Vol. 63, Issue 11, p. 1117). https://doi.org/10.1130/0016-7606(1952)63[1117:haaoet]2.0.co;2

Talchabhadel, R., Nakagawa, H., Kawaike, K., & Prajapati, R. (2020a). Evaluating the rainfall erosivity (R-factor) from daily rainfall data: an application for assessing climate change impact on soil loss in Westrapti River basin, Nepal. *Modeling Earth Systems and Environment*, *6*(3), 1741–1762. https://doi.org/10.1007/s40808-020-00787-w

Talchabhadel, R., Prajapati, R., Aryal, A., & Maharjan, M. (2020b). Assessment of rainfall erosivity (R-factor) during 1986–2015 across Nepal: a step towards soil loss estimation. *Environmental Monitoring and Assessment*, *192*, 293. https://doi.org/10.1007/s10661-020-8239-9

Tamrakar, N. (1999). Tectonic Developments and Slope Movements along the Surai Khola River, Siwalik Hills, Mid Western Nepal. MS Thesis. *Department of Geoscience, Shimane University, Matsue, Japan*.

Tamrakar, N. K., & Yokota, S. (2008). Types and processes of slope movements along East-West Highway, Surai Khola area, Mid-Western Nepal Sub-Himalaya. *Bulletin of the Department of Geology*, *11*, 1–4. https://doi.org/10.3126/bdg.v11i0.1427

Terranova, O., Antronico, L., Coscarelli, R., & Iaquinta, P. (2009). Soil erosion risk scenarios in the Mediterranean environment using RUSLE and GIS: An application model for Calabria (southern Italy). In *Geomorphology* (Vol. 112, Issues 3–4, pp. 228–245). https://doi.org/10.1016/j.geomorph.2009.06.009

Thiede, R. C., Bookhagen, B., Arrowsmith, J. R., Sobel, E. R., & Strecker, M. R. (2004). Climatic control on rapid exhumation along the Southern Himalayan Front. In *Earth and Planetary Science Letters* (Vol. 222, Issues 3–4, pp. 791–806). https://doi.org/10.1016/j.epsl.2004.03.015

Tiruwa, D. B., Khanal, B. R., Lamichhane, S., & Acharya, B. S. (2021). Soil erosion estimation using Geographic Information System (GIS) and Revised Universal Soil Loss Equation (RUSLE) in the Siwalik Hills of Nawalparasi, Nepal. *Journal of Water and Climate Change*, *12*(5), 1958–1974. https://doi.org/10.2166/wcc.2021.198

Tokuoka, T. (1992). The churiya (Siwalik) group in west central Nepal. *Bull. Dept. Geology, Tribhuvan Univ., Kathmandu, Nepal*, *2*(1), 75–87.

Tucker, C. J. (1979). Red and photographic infrared linear combinations for monitoring vegetation. *Remote Sensing of Environment*, *8*(2), 127–150. https://doi.org/10.1016/0034-4257(79)90013-0

Uddin, K., Murthy, M. S. R., Wahid, S. M., & Matin, M. A. (2016). Estimation of Soil Erosion Dynamics in the Koshi Basin Using GIS and Remote Sensing to Assess Priority Areas for Conservation. *PLOS ONE*, *11*(3), e0150494. https://doi.org/10.1371/journal.pone.0150494

Upreti, B. N. (1999). An overview of the stratigraphy and tectonics of the Nepal Himalaya. In *Journal of Asian Earth Sciences* (Vol. 17, Issues 5–6, pp. 577–606). https://doi.org/10.1016/s1367-9120(99)00047-4

Van der Knijff, J., Jones, R., & Montanarella, L. (1999). *Soil erosion risk assessment in Italy*.

Van Remortel, R. D., Hamilton, M. E., & Hickey, R. J. (2001). Estimating the LS Factor for RUSLE through Iterative Slope Length Processing of Digital Elevation Data within Arclnfo Grid. *Cartography*, *30*(1), 27–35. https://doi.org/10.1080/00690805.2001.9714133

Wei, W., Liu, Y., Zhang, L., & Li, L. (2024). Distribution assessment of soil erosion with revised RUSLE model in Tianshan Mountains. *Journal of Mountain Science*, *21*(3), 850–866. https://doi.org/10.1007/s11629-022-7881-9

Wischmeier, W. (1965). *Predicting rainfall-erosion losses from cropland east of the Rocky Mountains, Guide for selection of practices for soil and water conservation*.

Wischmeier, W. H., & Smith, D. D. (1978). *Predicting rainfall erosion losses: a guide to conservation planning*.

Yue-Qing, X., Xiao-Mei, S., Xiang-Bin, K., Jian, P., & Yun-Long, C. (2008). Adapting the RUSLE and GIS to model soil erosion risk in a mountains karst watershed, Guizhou Province, China. In *Environmental Monitoring and Assessment* (Vol. 141, Issues 1–3, pp. 275–286). https://doi.org/10.1007/s10661-007-9894-9